Author Manuscript

Author Manuscript

Author Manuscript

Author Manuscript

HHS Public Access

Author manuscript

Eur J Nucl Med Mol Imaging. Author manuscript; available in PMC 2022 February 01.

Published in final edited form as:

Eur J Nucl Med Mol Imaging. 2021 February ; 48(2): 383–394. doi:10.1007/s00259-020-04978-6.

Development of ^{89}Zr-Amivantamab bispecific to EGFR and c-MET for PET imaging of triple-negative breast cancer

Alessandra Cavaliere[1], **Suxia Sun**[1,2], **Supum Lee**[1], **Jacob Bodner**[1], **Ziqi Li**[1], **Yiyun Huang**[1], **Sheri L. Moores**[3], **Bernadette Marquez-Nostra**[1]

[1.]Department of Radiology and Biomedical Imaging. Yale University, New Haven, Connecticut, USA.

[2.]Department of Nutrition and Food Hygiene. Southern Medical University, Guangzhou, Guangdong, China.

[3.]Janssen Pharmaceutical. Philadelphia, PA, USA.

Abstract

Background: Amivantamab is a novel bispecific antibody that simultaneously targets the epidermal growth factor receptor (EGFR) and the hepatocyte growth factor receptor (HGFR/c-MET) that are overexpressed in several types of cancer including triple negative breast cancer (TNBC). Targeting both receptors simultaneously can overcome resistance to mono-targeted therapy. The purpose of this study is to develop ^{89}Zr-labeled Amivantamab as a potential companion diagnostic imaging agent to Amivantamab therapy using various preclinical models of TNBC for evaluation.

Methods: Amivantamab was conjugated to desferrioxamine (DFO) and radiolabeled with ^{89}Zr to obtain [^{89}Zr]ZrDFO-Amivantamab. Binding of the bispecific [^{89}Zr]ZrDFO-Amivantamab as well as its mono-specific “single arm” antibody controls were determined *in vitro* and *in vivo*. Biodistribution studies of [^{89}Zr]ZrDFO-Amivantamab were performed in MDA-MB-468 xenografts to determine the optimal imaging time point. PET/CT imaging with [^{89}Zr]ZrDFO-Amivantamab or its isotype control was performed in a panel of TNBC xenografts with varying levels of EGFR and c-MET expression.

Terms of use and reuse: academic research for non-commercial purposes, see here for full terms. http://www.springer.com/gb/open-access/authors-rights/aam-terms-v1

*Correspondence author: Bernadette Marquez-Nostra, PhD, Assistant Professor, Mailing address PET Center, Yale University, PO Box 208048, New Haven, CT 06520, Ph: (203)737-1376, bernadette.marquez-nostra@yale.edu.

Authors' contributions

AC, SS, SM, BMN contributed to the study conception and design. Material preparation and data collection were performed by AC, SS, SL, JB, ZL. All authors contributed to data analysis. The manuscript was written by AC, SL, JB and edited by BMN, SS, and YH. All authors reviewed and approved the manuscript.

Publisher's Disclaimer: This Author Accepted Manuscript is a PDF file of a an unedited peer-reviewed manuscript that has been accepted for publication but has not been copyedited or corrected. The official version of record that is published in the journal is kept up to date and so may therefore differ from this version.

Competing interests

Sheri Moores is an employee of Janssen Pharmaceuticals. The authors have declared that no competing interest exists.

Ethical approval

All applicable international, national, and institutional guidelines for the care and use of animals were followed.

Author Manuscript Author Manuscript Author Manuscript Author Manuscript

Results: [^{89}Zr]ZrDFO-Amivantamab was synthesized with a specific activity of 148 MBq/mg and radiochemical yield of ≥ 95%. Radioligand binding studies and western blot confirmed the order of EGFR and c-MET expression levels: HCC827 lung cancer cell (positive control) > MDA-MB-468 > MDA-MB-231 > MDA-MB-453. [^{89}Zr]Zr-DFO-Amivantamab demonstrated bispecific binding in cell lines co-expressed with EGFR and c-MET. PET/CT imaging with [^{89}Zr]ZrDFO-Amivantamab in TNBC xenografted mice showed Standard Uptake Value (SUV_{mean}) of 6.0 ± 1.1 in MDA-MB-468, 4.2 ± 1.4 in MDA-MB-231, and 1.5 ± 1.4 in MDA-MB-453 tumors, which are consistent with their receptors' expression levels on the cell surface.

Conclusion: We have successfully prepared a radiolabeled bispecific antibody, [^{89}Zr]ZrDFO-Amivantamab, and evaluated its pharmacologic and imaging properties in comparison with its single arm antibodies and non-specific isotype controls. [^{89}Zr]ZrDFO-Amivantamab demonstrated the greatest uptake in tumors co-expressing EGFR and c-MET.

Keywords

^{89}Zr; bispecific antibody; EGFR; c-MET; triple negative breast cancer

INTRODUCTION

The epidermal growth factor receptor (EGFR) and hepatocyte growth factor receptor, or cytoplasmic/mesenchymal epithelial transition factor (HGFR/c-MET), are two unique, closely linked tyrosine kinase receptors, in that inhibition of the signaling pathway for one receptor activates the other. Together they have been shown to synergistically mediate angiogenesis, progression, and motility in a wide variety of human cancers, including triple negative breast cancer (TNBC) [1, 2]. The EGFR and *MET* genes, which encode for the EGFR and c-MET proteins respectively, are amplified in the basal-like subtype of TNBC, resulting in the overexpression of the proteins [3]. EGFR and c-MET have been targeted independently for the treatment of breast cancer [4]. Resistance to mono-targeted treatments against EGFR or c-MET contributes to poor overall survival of patients with metastatic TNBC [5, 6]. On the contrary, preclinical studies in TNBC have shown that combination therapy with inhibitors of c-MET and EGFR have greater therapeutic efficacy compared with single agent treatments, highlighting the significance of the mechanistic cross-talk between EGFR and c-MET pathways [4].

A novel and alternative approach to combination therapies is the use of bispecific antibodies that can target two unique antigens. Bispecific antibody therapeutics offer the advantages of improved efficacy, enhanced tumor specificity, and reduced cytotoxicity [7]. Amivantamab (JNJ-61186372) is a human bispecific antibody engineered to target both human EGFR and c-MET simultaneously for the treatment of advanced non-small cell lung cancer (NSCLC) [8]. Amivantamab inhibits and degrades both EGFR and c-MET in NSCLC xenografts more potently than single agent inhibition of either receptor, or combination treatments targeting both receptors [9, 10]. Further, Amivantamab is also engineered with low fucosylation to elicit enhanced antibody-dependent cell-mediated cytotoxicity (ADCC) to kill cancer cells [11].

Author Manuscript Author Manuscript Author Manuscript Author Manuscript

Amivantamab is currently in Phase I clinical trial for the treatment of patients with metastatic NSCLC [8, 12]. This novel antibody has the potential to be clinically translated to the basal-like subtype of TNBC, given the overexpression of EGFR and c-MET as discussed above. Thus, patient selection for Amivantamab therapy is needed. Current diagnostic techniques to screen patients eligible for targeted therapy rely on tissue biopsy. An example is immunohistochemical (IHC) examination of biopsied tissue, which has several limitations. Improper specimen fixation, tissue pre-treatment and processing, antigen degradation, and subjective staining quantification are frequent and can therefore affect the proper selection of patients for treatment [13, 14]. Moreover, detection of c-MET is particularly challenging due to a limited choice of reproducible and properly validated antibodies to c-MET [15, 16]. One way to overcome the limitations of IHC is through the use of companion diagnostic agents (CDx), which are imaging biomarkers that could help predict response to corresponding therapeutic drugs. Positron Emission Tomography (PET) imaging CDx can provide information on the biodistribution of the related therapeutic agents and determine antigen expression throughout the whole body in a non-invasive way [17, 18]. In particular, PET imaging with ^{89}Zr-labeled antibodies has been increasingly used as a non-invasive tool to select patients likely to respond to antibody treatments [17].

Molecular imaging technique has been applied to bispecific constructs such as antibodies [19, 20], antibody heterodimers [21, 22], peptides, and nanoparticles [23]. Yet, no molecular imaging probe has been developed to target the cross-talk between EGFR and c-MET. Considering the overexpression of EGFR and c-MET in TNBC, the aim of this study is to re-purpose Amivantamab for TNBC by developing ^{89}Zr-labeled Amivantamab as a PET CDx to assess the combined expression of EGFR and c-MET, as well as the delivery of Amivantamab to TNBC tumors. Thus, ^{89}Zr-labeled Amivantamab could be used as a PET imaging CDx to select patients most likely to benefit from Amivantamab treatment for TNBC and other types of cancer driven by the overexpression of EGFR and c-MET. Herein, we report the synthesis and evaluation of ^{89}Zr-labeled Amivantamab in preclinical models of TNBC.

MATERIALS AND METHODS

Cell lines

All cell lines were purchased from the American Type Culture Collection (ATCC, Manassas, VA) and cultured following supplier instructions. Cell lines were authenticated by ATCC before and after our studies using short tandem repeat (STR) profiling.

Western blot

EGFR and c-MET expression in cell lines was validated by western blotting using their respective primary antibodies (rabbit anti-human EGFR and mouse anti-human MET; Cell Signaling Technology, 1:1000). Secondary antibodies (goat anti-rabbit IgG-HRP and goat anti-mouse IgG-HRP; Cell Signaling Technology, 1:3000) followed by the SuperSignal® West Pico Chemiluminescent Substrate (Thermo-Scientific) were applied. Bands corresponding to each receptor were quantified based on pixel intensity and normalized to

Author Manuscript Author Manuscript Author Manuscript Author Manuscript

those from the β-actin control using G:Box 9 (Syngene). Detailed procedures are described in the Supplementary Material.

Preparation of radiopharmaceuticals

Amivantamab, IgG1 isotype control, and single arm α-EGFR and α-c-MET antibodies were provided by Janssen Pharmaceuticals [9]. Briefly, antibodies were buffer-exchanged with 0.1 M sodium bicarbonate buffer pH 7.5 and conjugated with a 5-fold molar excess of DFO-Bz-NCS (Macrocyclics, Inc.). The DFO-antibody conjugates were radiolabeled with neutralized [^{89}Zr]Zr-oxalate (Washington University in St. Louis or 3D Imaging) in 0.25 M HEPES (pH 7.1) and purified via buffer-exchange in PBS (pH 7.4). These parameters were the best conditions we found that maintained the stability, protein integrity, and high specific activity of the radiolabeled Amivantamab. Details of the chromatographic analyses and stability studies are described in the Supplementary Material.

Quantification of DFO:Amivantamab ratio

The number of chelators per Amivantamab was determined using a radioisotopic dilution assay as previously described [24]. Briefly, DFO-Amivantamab (6.7 μM) was incubated with increasing concentrations of $FeCl_3$ ranging from 1.5 to 25 μM at 4°C for 16 h. The neutralized [^{89}Zr]Zr-Oxalate was then added and incubated for 1 h at 37°C to bind to unlabeled DFO sites. The percentage of intact [^{89}Zr]ZrDFO-Amivantamab was determined via radio-TLC. Data were analyzed as previously described [24]. This experiment was performed three times.

Determination of binding affinity and immunoreactivity

The binding affinity of [^{89}Zr]ZrDFO-Amivantamab and its mono-specific single arm antibody controls ([^{89}Zr]ZrDFO-α-EGFR and [^{89}Zr]ZrDFO-α-c-MET) were determined on immobilized EGFR-ECD-Fc or c-MET-ECD-Fc (R&D Systems) recombinant proteins (Detailed procedures are described in the Supplementary Material). Immunoreactivity was determined via a competitive binding assay between [^{89}Zr]ZrDFO-Amivantamab and varying concentrations of either DFO-conjugated or unconjugated Amivantamab, following previous methods [24]. The IC_{50} values of [^{89}Zr]ZrDFO-Amivantamab were determined for MDA-MB-468 and MDA-MB-231 TNBC cell lines, as well as for HCC827 lung cancer cell line (positive control). Competitive binding assays on these cell lines were performed between [^{89}Zr]ZrDFO-Amivantamab and varying concentrations of DFO-Amivantamab, following published procedures [19].

Cell binding/blocking and internalization studies

The HCC827, MDA-MB-468, and MDA-MB-231 cell lines co-express EGFR and c-MET while MDA-MB-453 lacks expression of these receptors [4]. The specificity of [^{89}Zr]ZrDFO-Amivantamab was determined in these cell lines following a previously reported method [24]. The final concentration of each blocking agent (Amivantamab, α-EGFR, or α-c-MET) was 100 μg/mL. [^{89}Zr]ZrDFO-Amivantamab was then added at a final concentration of 16 ng/mL and incubated at 2 h at 37°C. The percentage of radioactivity bound per million cells was calculated. The rate of cellular internalization for [^{89}Zr]ZrDFO-

Author Manuscript Author Manuscript Author Manuscript Author Manuscript

Amivantamab was determined in MDA-MB-468 and MDA-MB-231 cell lines, following our established method [24].

Determination of cell membrane expression of EGFR and c-MET

The cell membrane expression of EGFR and c-MET was evaluated in the MDA-MB-468, MDA-MB-231, and HCC827 cell lines via binding of [^{89}Zr]ZrDFO-α-EGFR or [^{89}Zr]ZrDFO-α-c-MET single arm antibodies at 0°C. For each cell line, 1 × 10^6 cells in 0.5 mL of PBS were placed into microcentrifuge tubes in triplicates. A solution (200 μL at 16 ng/mL concentration) of either [^{89}Zr]ZrDFO-α-EGFR or [^{89}Zr]ZrDFO-α-c-MET in 1% BSA in PBS was added and incubated for 2 h at 0°C with gentle rocking. Cells were centrifuged for 2 min at 600 × g at 4°C. The supernatant was aspirated, and the pellet was washed twice with 1 mL of ice-cold PBS. Cells were treated with acidic buffer to separate the supernatant (membrane-bound radioactive fraction) from the cell pellet (internalized fraction), as described previously [24]. Radioactivity was assayed in a gamma counter and the percentage of radioactivity bound per million cells was calculated.

Animal Models

All animal studies were performed in accordance with a protocol approved by the Institutional Animal Care and Use Committee. Female athymic nude mice (5 - 8 weeks old) were obtained from Charles River Laboratories. Xenografts were generated by inoculating mice with 100 μL of 5 × 10^6 MDA-MB-468 or MDA-MB-453 cells and 1 × 10^6 MDA-MB-231 cells suspended in 30% Matrigel© Basement Membrane Matrix (Corning) in PBS. Tumor volumes were calculated as follows: length × width × height × 0.5. Studies were conducted when tumor sizes reached 100 – 500 mm^3 at 4 weeks post inoculation for MDA-MB-468 and MDA-MB-453 xenografts, and at 2 weeks for MDA-MB-231.

Biodistribution studies

Biodistribution studies of [^{89}Zr]ZrDFO-Amivantamab were performed in mice bearing the MDA-MB-468 xenografts. [^{89}Zr]ZrDFO-Amivantamab (0.37 MBq, with specific activity of 37 MBq/mg) was injected via the tail vein. Animals were euthanized and tissues were harvested, weighed, and assayed in a gamma counter at 6 h and at 1, 2, 3, 4, and 7 days post injection (p.i.) (n = 3 per time point). The percentage of injected dose per gram of organ (%ID/g) was calculated. Additional cohorts of animals (n = 3 per group) were injected with [^{89}Zr]ZrDFO-α-EGFR or [^{89}Zr]ZrDFO-α-c-MET at similar dose and specific activity as [^{89}Zr]ZrDFO-Amivantamab. Animals were euthanized at 4 days p.i. and biodistribution study was performed. The uptake of each ^{89}Zr-labeled antibody (%ID/g) in the tumor was compared. For the blocking study, a separate cohort of animals (n = 3) received 200-fold excess (20 mg/kg) of unlabeled Amivantamab or its single arm antibodies at one day prior to injection of [^{89}Zr]ZrDFO-Amivantamab. Animals were euthanized at 4 days thereafter. The uptake of [^{89}Zr]ZrDFO-Amivantamab in the tumor under blocking conditions was compared with that of the non-blocking condition.

Author Manuscript Author Manuscript Author Manuscript Author Manuscript

PET imaging experiments

For small animal PET imaging, mice were anesthetized using isoflurane (1.5 - 2% v/v in O_2). A radioactivity dose of 1.85 MBq of [^{89}Zr]ZrDFO-Amivantamab (specific activity = 148 MBq/mg) or [^{89}Zr]ZrDFO-IgG1 (specific activity = 37 MBq/mg) was injected via the tail vein. PET/CT imaging was performed at 4 days p.i. Static PET images were acquired for 10 min followed by CT image acquisition using an Inveon PET/CT scanner (Siemens, Knoxville, TN). Images were reconstructed using an ordered subset expectation maximization (OSEM-3D) algorithm and co-registered with CT images using the Inveon Research Workplace Workstation software (Siemens). Regions of interest (ROI) were drawn on the tumor region and the uptake of the radiolabeled antibody was quantified by calculating the mean standardized uptake values (SUV_{mean}) from decay-corrected ROI activity concentrations. Biodistribution studies were conducted post-PET imaging as described above.

Immunohistochemistry analysis

Tissue sections were subjected to c-MET and EGFR staining on Leica Bond Rx using Leica Refine Polymer Detection Kit. Sections were baked, dewaxed, and rehydrated. Antigen retrieval was performed using ER2 for 20 min at 100°C. Peroxide block was added followed by primary c-MET (0.1 μg/mL) or EGFR (0.17 μg/mL) antibody for 1 h. Post primary reagent was added for 8 min followed by Polymer for another 8 min. Mixed DAB Refine was added to slides and finally counterstained with Hematoxylin.

Statistical evaluation

Data were analyzed using GraphPad Prism version 7.01 (GraphPad Software Inc., La Jolla, CA) and expressed as mean ± S.D. A one-way ANOVA was used to analyze data with one variable and a two-way ANOVA for data with two variables. Tukey's test was used for post-hoc analysis. $P < 0.05$ was considered statistically significant.

RESULTS

Synthesis and characterization of radiopharmaceuticals

[^{89}Zr]ZrDFO-Amivantamab was synthesized with a specific activity of 148 MBq/mg, and radiochemical yield of ≥ 95% (Fig. S1a). Protein aggregation analysis determined that Amivantamab had ≥ 98% monomer (Fig. S1b and S1c). The ratio of DFO : Amivantamab was determined to be 5 ± 1, which is in agreement with the stoichiometric ratio used during the conjugation (Fig. 1). In PBS medium, [^{89}Zr]ZrDFO-Amivantamab was stable up to 24 h with 87 ± 1.5% of intact monomer (Fig. 2). Representative HPLC chromatogram from this study is shown in Fig. S2a. The radiopharmaceutical had greater stability in mouse serum than in human serum up to 4 days post synthesis, with 87 ± 2.1 and 70 ± 3% of intact monomer, respectively (Fig. 2). Representative HPLC chromatograms from these studies are shown in Fig. S2b and c. The same conjugation and labeling conditions were applied for the control antibodies: IgG1, and single arm α-EGFR and α-c-MET. Under those conditions, the control antibodies were all labeled with ^{89}Zr with a specific activity of 37 MBq/mg in ≥ 95% radiochemical yield and ≥ 90% monomer.

Author Manuscript Author Manuscript Author Manuscript Author Manuscript

Specificity of [^{89}Zr]ZrDFO-Amivantamab *in vitro*

First, we validated the expression of EGFR and c-MET in a panel of TNBC cell lines via western blotting using HCC827 lung cancer cell line as a positive control for co-expression of both receptors (Fig. 3). MDA-MB-468, MDA-MB-231, and MDA-MB-453 cell lines were confirmed to have high, medium, and very low expression, respectively, of both EGFR and c-MET proteins. These results confirmed the suitability of using these cell lines, with varying degrees of EGFR and c-MET expression, for the *in vitro* and *in vivo* studies with [^{89}Zr]ZrDFO-Amivantamab.

We characterized the binding properties of [^{89}Zr]ZrDFO-Amivantamab in all cell lines described above (Fig. 4). The specificity of [^{89}Zr]ZrDFO-Amivantamab for EGFR and c-MET was determined by blocking with a 200-fold excess of unlabeled Amivantamab or its single arm antibody controls following our previous method [24]. Under non-blocking conditions, the percentage of [^{89}Zr]ZrDFO-Amivantamab bound per million cells was found to be 119 ± 20, 72 ± 1.8, 29 ± 0.3, and 0.4 ± 0.04%, respectively, for HCC827, MDA-MB-468, MDA-MB-231, and MDA-MB-453 (Fig. 4). Blocking with the unlabeled Amivantamab significantly decreased the binding of the [^{89}Zr]ZrDFO-Amivantamab by > 96% across the double-positive cell lines (HCC827, MDA-MB-468, and MDA-MB-231, $p < 0.0001$). Blocking with the unlabeled α-EGFR or α-c-MET, decreased radioligand binding by > 41% ($p < 0.001$) and > 19% ($p \leq 0.05$), respectively, across the double positive cell lines. [^{89}Zr]ZrDFO-Amivantamab displayed ≥ 25% greater binding under c-MET blocking conditions (EGFR-specific) as compared with EGFR blocking (c-MET-specific) ($p < 0.01$). This result suggests greater EGFR expression over c-MET, which is consistent with the results obtained by western blotting (Fig. 3). Overall, [^{89}Zr]ZrDFO-Amivantamab demonstrated high specificity for all cell lines co-expressed with EGFR and c-MET.

Determination of binding affinity, immunoreactivity, and rate of internalization

We confirmed the retention of bispecific binding and binding affinity of [^{89}Zr]ZrDFO-Amivantamab by quantifying the radioligand equilibrium dissociation constant (K_D) for each of the extracellular domain proteins EGFR and c-MET using saturation binding assays. [^{89}Zr]ZrDFO-Amivantamab was found to have K_D value of 9.9 ± 2.1 nM for EGFR and 16.9 ± 5.9 nM for c-MET (Fig. 5a and b, respectively). Then, we determined the binding affinity of the two radiolabeled single arm antibodies, which bind to either EGFR or c-MET in a monovalent fashion. [^{89}Zr]ZrDFO-α-EGFR and [^{89}Zr]ZrDFO-α-c-MET showed similar nanomolar affinity for their target proteins with K_D values of 8.4 ± 1.7 nM and 4.2 ± 1.5 nM, respectively (Fig. 5c and d). These results confirmed that the Fab arms of [^{89}Zr]ZrDFO-Amivantamab retain binding affinities for the target proteins and are similar to those displayed by the ^{89}Zr-labeled single arm antibody controls for their separate target.

We further determined the retained immunoreactivity of the [^{89}Zr]ZrDFO-Amivantamab conjugate by competitive binding with varying concentrations of either the DFO-Amivantamab conjugate or parent Amivantamab in EGFR and c-MET proteins. Competition with DFO-Amivantamab yielded IC_{50} values of 7.5 nM for EGFR and 3.7 nM for c-MET (Fig. S3a). In comparison, the IC_{50} values of parent Amivantamab were determined to be 4.3 nM for EGFR and 1.3 nM for c-MET (Fig. S3b). Thus, the ratios of IC_{50} values for

Author Manuscript Author Manuscript Author Manuscript Author Manuscript

conjugate : parent for EGFR and c-MET were determined to be 1.7 and 2.8, respectively. These results confirm preservation of antigen-binding after DFO conjugation.

We next measured the IC_{50} values of [^{89}Zr]ZrDFO-Amivantamab in cell lines co-expressing EGFR and c-MET by competition with varying concentrations of DFO-Amivantamab to further evaluate its affinity for these cell lines *in vitro*. IC_{50} values were determined to be 23.6, 7.2 and 3.9 nM for MDA-MB-468, MDA-MB-231, and HCC827, respectively (Fig. S4).

Given that cellular internalization is part of the mechanism by which Amivantamab degrades EGFR and c-MET, we measured the rate of cellular internalization by [^{89}Zr]ZrDFO-Amivantamab in TNBC cell lines co-expressing EGFR and c-MET using our established method [24]. At 18 h after incubation, 40% of the bound [^{89}Zr]ZrDFO-Amivantamab internalized in MDA-MB-468 cells, and 55% in MDA-MB-231 cells (Fig. 6a and b). Control reactions were performed at 4°C, to reduce the rate of receptor-mediated internalization [25]. As expected, the rate of cellular internalization was significantly reduced in both cell lines ($p < 0.001$) at 4°C.

Validation of cell membrane expression of EGFR and c-MET

Given that the therapeutic efficacy of Amivantamab is due to its binding to both EGFR and c-MET on the cancer cell surface, we determined the cell surface expression of these receptors in the double positive cell lines. Radioligand binding was performed at 0°C to prevent receptor-mediated internalization. Cell surface binding was quantified by measuring the bound radioactivity, separately, on the cell membrane and the internalized fraction. Binding of [^{89}Zr]ZrDFO-α-EGFR and [^{89}Zr]ZrDFO-α-c-MET was found to be predominantly on the cell surface (Fig. 7). The surface-bound fractions of [^{89}Zr]ZrDFO-α-EGFR were 7.1 ± 0.4, 17.9 ± 2.7 and 4.2 ± 1.4% per million cells for HCC827, MDA-MB-468, and MDA-MB-231 cells, respectively, while those of [^{89}Zr]ZrDFO-α-c-MET were 9.5 ± 2.2, 6.6 ± 0.8, 2.9 ± 0.9% per million cells, respectively (Fig. 7). Internalized fractions were negligible across ah the cell lines (< 0.1%).

Pharmacokinetic properties of [^{89}Zr]ZrDFO-Amivantamab

The pharmacokinetic properties of [^{89}Zr]ZrDFO-Amivantamab were evaluated by biodistribution studies in mice bearing the MDA-MB-468 xenografts. The highest tumor uptake was reached at 4 days p.i. with 38 ± 14%ID/g and decreased to 21 ± 11%ID/g at 7 days p.i., although not significantly ($p = 0.85$, Fig. 8). The highest tumor-to-blood (5 ± 4.9) and tumor-to-muscle (43 ± 35) ratios were also observed at 4 days p.i. [^{89}Zr]ZrDFO-Amivantamab uptake in normal organs such as liver and spleen was considerably lower (< 15%ID/g) than that in the tumor and reached steady-state from 2 days p.i. onward. The uptake in the bone increased over time, from 2.7 ± 1.1%ID/g at 6 h p.i. to 8.9 ± 7.2%ID/g at 7 days p.i., likely due to de-complexation of ^{89}Zr from the conjugate as confirmed by the serum stability studies (Fig. 2) and other studies reported previously [26]. A complete biodistribution profile of the [^{89}Zr]ZrDFO-Amivantamab in all organs over time is provided in Table S1. Based on the results from these biodistribution and stability studies, we chose to image the xenografts at 4 days p.i. of [^{89}Zr]ZrDFO-Amivantamab or its isotype control.

Author Manuscript Author Manuscript Author Manuscript Author Manuscript

In vivo binding specificity of [^{89}Zr]ZrDFO-Amivantamab in the MDA-MB-468 xenografts

To determine the *in vivo* binding specificity of [^{89}Zr]ZrDFO-Amivantamab, we performed a blocking study in mice bearing the MDA-MB-468 xenografts. Results are presented in Fig. 9a. Blocking EGFR and c-MET simultaneously with the unlabeled Amivantamab (200-fold excess, 20 mg/kg) significantly reduced the tumor uptake of [^{89}Zr]ZrDFO-Amivantamab by 60% ($p = 0.04$). When blocking the EGFR receptor using the α-EGFR single arm antibody, the uptake of the [^{89}Zr]ZrDFO-Amivantamab decreased by 37% ($p = 0.3$). When blocking the c-MET receptor with the α-c-MET single arm antibody, there was no change in the uptake of [^{89}Zr]ZrDFO-Amivantamab in tumor ($p = 0.9$). We further investigated the effect of the dose of the blocking antibody on receptor expression *in vivo* by conducting an independent study, where a separate cohort of MDA-MB-468 xenografts were injected with 20 mg/kg of unlabeled Amivantamab, α-c-MET or α-EGFR. After 24 h, tumors were harvested, lysed, and protein lysates were analyzed by Western blot to determine the expression levels of EGFR and c-MET. We observed reduced expression of both receptors with the 20 mg/kg dose of all antibodies (Fig. S5). These results confirm that MDA-MB-468 xenografts are especially sensitive to treatment with the blocking dose of all antibodies in this study. This therapeutic effect could have altered the tumor vasculature and therefore affected the uptake of [^{89}Zr]ZrDFO-Amivantamab. Thus, we evaluated the specificity of [^{89}Zr]ZrDFO-Amivantamab in the MDA-MB-468 xenografts in a different way. We compared the tumor uptake of [^{89}Zr]ZrDFO-Amivantamab with those of the radiolabeled single arm antibodies, [^{89}Zr]ZrDFO-α-EGFR and the [^{89}Zr]ZrDFO-α-c-MET, as these control antibodies are derived from the Amivantamab structure but bind monovalently to their respective targets. The tumor uptake of [^{89}Zr]ZrDFO-Amivantamab was found to be significantly higher than that of the single arm [^{89}Zr]ZrDFO-α-EGFR ($p < 0.05$) or [^{89}Zr]ZrDFO-α-c-MET ($p < 0.01$) (Fig. 9b). These results provided another piece of evidence for the binding of [^{89}Zr]ZrDFO-Amivantamab to both EGFR and c-MET *in vivo*.

PET imaging with [^{89}Zr]ZrDFO-Amivantamab

Our goal was to validate the feasibility of [^{89}Zr]ZrDFO-Amivantamab as a companion diagnostic imaging agent. PET imaging with [^{89}Zr]ZrDFO-Amivantamab was performed in the TNBC xenografts to determine whether we could discriminate among different levels of both EGFR and c-MET expression. The imaging quality produced by [^{89}Zr]ZrDFO-Amivantamab was compared with that of the radiolabeled antibody isotype control, [^{89}Zr]ZrDFO-IgG1. PET imaging showed greater tumor accumulation of [^{89}Zr]ZrDFO-Amivantamab in MDA-MB-468 and MDA-MB-231 than [^{89}Zr]ZrDFO-IgG1 with excellent imaging contrast (Fig. 10a). [^{89}Zr]ZrDFO-Amivantamab had a 1.4-fold higher SUV_{mean} in the MDA-MB-468 tumors ($n = 3$; $SUV_{mean} = 6.0 \pm 1.1$) than in the MDA-MB-231 ($n = 4$; $SUV_{mean} = 4.2 \pm 1.4$; $p = 0.04$), and a 4-fold higher uptake than in the MDA-MB-453 ($n = 6$; $SUV_{mean} = 1.5 \pm 1.4$; $p < 0.0001$) (Fig. 10b). Furthermore, the imaging studies showed 5-fold ($p < 0.0001$) and 3-fold ($p < 0.01$) higher tumor specificity of [^{89}Zr]ZrDFO-Amivantamab than [^{89}Zr]ZrDFO-IgG1 in the MDA-MB 468 and MDA-MB-231 models, respectively (Fig. 10c).

Post-PET biodistribution studies corroborated the PET imaging results, showing that the tumor uptake of [^{89}Zr]ZrDFO-Amivantamab in the MDA-MB-468 model was 1.7-fold and

Author Manuscript Author Manuscript Author Manuscript Author Manuscript

3.5-fold higher, respectively, than those in the MDA-MB-231 ($p < 0.0001$) and MDA-MB-453 models ($p < 0.0001$). Similar uptake levels in normal organs were observed among the three groups (Fig. 11). Results from the tumor uptake of [^{89}Zr]ZrDFO-Amivantamab *in vivo* were consistent with those from radioligand binding assays *in vitro* (Fig. 4). However, results from *ex vivo* immunohistochemistry (IHC) analyses were discordant with PET imaging and western blot data, as IHC could not delineate the differences in EGFR and c-MET expression between MDA-MB-468 and MDA-MB-231 xenografts (Fig. 12).

DISCUSSION

Non-invasive imaging of targeted therapies have the potential to predict treatment outcome and overcome limitations with biopsy-based diagnostic tools [17]. CDx agents of bispecific antibodies targeting antigens on cancer cells [19] and eliciting contact between T-cells and cancer cells [20] have recently been developed as PET imaging probes and successfully evaluated preclinically in cancer models. These studies highlight the need for CDx of promising new therapeutic bispecific antibodies to potentially select patients likely to respond to these novel therapeutics. In the current study, we developed [^{89}Zr]ZrDFO-Amivantamab as a CDx PET agent to quantitatively measure the combined expression levels of EGFR and c-MET in TNBC xenografts.

Our radioligand binding study confirmed the specificity of [^{89}Zr]ZrDFO-Amivantamab for both EGFR and c-MET *in vitro* in a panel of TNBC cell lines that overexpress more EGFR than c-MET (Fig. 4). Our saturation assay results suggest similar binding affinity of [^{89}Zr]ZrDFO-Amivantamab for EGFR and c-MET (Fig. 5a and b). We showed that [^{89}Zr]ZrDFO-Amivantamab binding was consistent with the levels of EGFR but not c-MET expression, as determined by western blotting (Fig. 3). In comparison, we quantified the relative *in vitro* expression of EGFR and c-MET in our blocking studies of [^{89}Zr]ZrDFO-Amivantamab with either α-EGFR (c-MET-specific) or α-c-MET (EGFR-specific), respectively (Fig. 4). The binding of [^{89}Zr]ZrDFO-Amivantamab in the double positive cell lines under these blocking conditions was consistent with the results from the cell membrane binding of the ^{89}Zr-labeled single arm antibodies (Fig. 7). The latter indicated that the MDA-MB-468 and MDA-MB-231 cell lines exhibited much lower levels of c-MET expression on the cell membrane. These results suggest that binding of [^{89}Zr]ZrDFO-Amivantamab in these TNBC cell lines might be driven primarily by EGFR due to greater EGFR density on MDA-MB-468 *in vitro*. However, our study is limited by the absence of TNBC cell lines over-expressing more c-MET than EGFR.

Interestingly, our cellular internalization study shows different rates of internalization for [^{89}Zr]ZrDFO-Amivantamab across cell lines (Fig 6a and b). A prolonged cell surface retention time of [^{89}Zr]ZrDFO-Amivantamab in the MDA-MB-468 model could signify increased antibody-mediated effector functions such as antibody-dependent cellular cytotoxicity (ADCC) *in vivo* and positively impact therapy outcome in this model as compared to the MDA-MB-231 model, which is characterized by a faster internalization rate. However, part of the mechanism of response is also cellular internalization of Amivantamab followed by degradation of EGFR and c-MET. Future studies are warranted to

Author Manuscript Author Manuscript Author Manuscript Author Manuscript

evaluate the relationship between rates of internalization and response to Amivantamab treatment.

We compared the tumor uptake of [^{89}Zr]ZrDFO-Amivantamab with that of its ^{89}Zr-labeled single arm antibodies from which Amivantamab is structurally-derived. Since the control antibodies were also chemically modified with the DFO chelate, we confirmed that the binding affinity of [^{89}Zr]ZrDFO-Amivantamab for EGFR and c-MET was similar to those of [^{89}Zr]ZrDFO-α-EGFR and [^{89}Zr]ZrDFO-α-c-MET controls (Fig. 5a and b and Fig. 5c and d, respectively). In a biodistribution study using the MDA-MB-468 xenografts, [^{89}Zr]ZrDFO-Amivantamab gave significantly highest uptake in the tumor than either the [^{89}Zr]ZrDFO-α-EGFR or [^{89}Zr]ZrDFO-α-c-MET (Fig. 9b), indicating the bispecific binding nature of [^{89}Zr]ZrDFO-Amivantamab for both EGFR and c-MET *in vivo*. Additionally, the greater tumor uptake of [^{89}Zr]ZrDFO-α-EGFR compared with that of [^{89}Zr]ZrDFO-α-c-MET (Fig. 9b) corroborates the greater cell surface expression of EGFR than c-MET in this tumor model. This result is confirmed by our cell membrane binding study of these ^{89}Zr-labeled single arm antibodies *in vitro* (Fig. 7). However, it remains to be determined, in a putative TNBC model overexpressing more c-MET than EGFR, which of the Fab arms of [^{89}Zr]ZrDFO-Amivantamab contributes more to the binding and overall tumor uptake of [^{89}Zr]ZrDFO-Amivantamab *in vivo*. To this end, future studies will evaluate [^{89}Zr]ZrDFO-Amivantamab in other types of cancer driven by the overexpression of EGFR and c-MET.

We determined the sensitivity of [^{89}Zr]ZrDFO-Amivantamab to image EGFR and c-MET co-expression *in vivo*. PET imaging with [^{89}Zr]ZrDFO-Amivantamab delineated significant differences in uptake among tumor models with high, moderate, and low expression levels of EGFR and c-MET (Fig. 10a and b). In contrast with results from PET imaging studies, radioligand binding assays, and independent biochemical measurements, IHC assays did not detect a difference in either EGFR or c-MET expression between the highly positive MDA-MB-468 and the moderate MDA-MB-231 tumors (Fig. 12). This discrepancy could be due to the limitations of IHC to accurately quantify total protein expression [13]. Thus, PET imaging of [^{89}Zr]ZrDFO-Amivantamab appears to be a more sensitive and reliable technique to quantify total expression of EGFR and c-MET in tumors than the “gold standard” IHC method currently used in the clinic for screening patients eligible for targeted therapies. While the efficacy of Amivantamab in the treatment of TNBC remains to be evaluated, our results suggest that PET imaging with the CDx agent [^{89}Zr]ZrDFO-Amivantamab may be an effective and reliable tool to assess the total expression levels of the EGFR and c-MET proteins in TNBC and select the patients likely to respond to Amivantamab treatment. Efficacy studies of the Amivantamab in TNBC models and companion imaging with [^{89}Zr]ZrDFO-Amivantamab are warranted to further correlate pre-treatment imaging to response to therapy.

Lastly, Amivantamab, like most antibody therapeutics in the market, has no cross-reactivity to murine homologues of EGFR and c-MET. Thus, our studies do not reflect comparable biodistribution in humans. Toxicity cannot be evaluated in our studies, which is an inherent limitation for all antibodies that only bind to human antigens with no cross-reactivity to the species investigated preclinically. However, previous studies have shown that Amivantamab

Author Manuscript Author Manuscript Author Manuscript Author Manuscript

has no toxicity in non-human primates [9]. Our preclinical study demonstrates the ability of [^{89}Zr]ZrDFO-Amivantamab to differentiate the gradations of total EGFR and c-MET co-expression in various tumor xenograft models. These results provide evidence for the specificity and sensitivity of [^{89}Zr]ZrDFO-Amivantamab *in vivo* and its potential to be used as a companion diagnostic imaging agent for Amivantamab therapy.

CONCLUSIONS

Our current studies demonstrate the ability of non-invasive imaging with [^{89}Zr]ZrDFO-Amivantamab to detect the total levels of EGFR and c-MET expression in TNBC tumors with high specificity. This CDx has the potential to be used in clinical research to stratify patients eligible for Amivantamab therapy in TNBC or other types of cancer primarily driven by EGFR and c-MET.

Supplementary Material

Refer to Web version on PubMed Central for supplementary material.

Acknowledgments

We thank the Yale PET Center for the use of the small animal PET/CT scanner, Washington University in St. Louis and 3D Imaging LLC for the production of ^{89}Zr-oxalate, and Yale Pathology Translational Services for the immunohistochemical analyses.

Funding

This research was funded by the Lion Hearts. Mr. Lee, Dr. Cavaliere and Dr. Marquez-Nostra are supported in part by the NCI R00 CA201601.

REFERENCES

1. Chae YK, Gagliato Dde M, Pai SG, Carneiro B, Mohindra N, Giles FJ, et al. The Association between EGFR and cMET Expression and Phosphorylation and Its Prognostic Implication in Patients with Breast Cancer. PLoS One. 2016;11(4). doi: 10.1371/journal.pone.0152585.
2. Puri N, Salgia R. Synergism of EGFR and c-Met pathways, cross-talk and inhibition, in non-small cell lung cancer. J Carcinog. 2008;7:9. doi: 10.4103/1477-3163.44372. [PubMed: 19240370]
3. Lehmann BD, Bauer JA, Chen X, Sanders ME, Chakravarthy AB, Shyr Y, et al. Identification of human triple-negative breast cancer subtypes and preclinical models for selection of targeted therapies. J Clin Invest. 2011;121(7):2750–67. doi: 10.1172/JCI45014. [PubMed: 21633166]
4. Linklater ES, Tovar EA, Essenburg CJ, Turner L, Madaj Z, Winn ME, et al. Targeting MET and EGFR crosstalk signaling in triple-negative breast cancers. Oncotarget. vol 432016 p. 69903–15.
5. Carey LA, Rugo HS, Marcom PK, Mayer EL, Esteva FJ, Ma CX, et al. TBCRC 001: randomized phase II study of cetuximab in combination with carboplatin in stage IV triple-negative breast cancer. J Clin Oncol. 2012;30(21):2615–23. doi: 10.1200/JCO.2010.34.5579. [PubMed: 22665533]
6. Dieras V, Campone M, Yardley DA, Romieu G, Valero V, Isakoff SJ, et al. Randomized, phase II, placebo-controlled trial of onartuzumab and/or bevacizumab in combination with weekly paclitaxel in patients with metastatic triple-negative breast cancer. Ann Oncol. 2015;26(9):1904–10. doi: 10.1093/annonc/mdv263. [PubMed: 26202594]
7. Labrijn AF, Janmaat ML, Reichert JM, Parren PWHI. Bispecific antibodies: a mechanistic review of the pipeline. Nature Reviews Drug Discovery. 2019;18(8):585–608. doi: doi:10.1038/s41573-019-0028-1. [PubMed: 31175342]

Author Manuscript Author Manuscript Author Manuscript Author Manuscript

8. Study of JNJ-61186372, a Human Bispecific EGFR and cMet Antibody, in Participants With Advanced Non-Small Cell Lung Cancer - Tabular View - ClinicalTrials.gov. https://clinicaltrials.gov/ct2/show/record/NCT02609776 (2020). Accessed.
9. Moores SL, Chiu ML, Bushey BS, Chevalier K, Luistro L, Dorn K, et al. A Novel Bispecific Antibody Targeting EGFR and cMet Is Effective against EGFR Inhibitor-Resistant Lung Tumors. Cancer Res. 2016;76(13):3942–53. doi: 10.1158/0008-5472.can-15-2833. [PubMed: 27216193]
10. Kontermann RE, Brinkmann U. Bispecific antibodies. Drug Discov Today. 2015;20(7):838–47. doi: 10.1016/j.drudis.2015.02.008. [PubMed: 25728220]
11. Grugan KD, Dorn K, Jarantow SW, Bushey BS, Pardinas JR, Laquerre S, et al. Fc-mediated activity of EGFR x c-Met bispecific antibody JNJ-61186372 enhanced killing of lung cancer cells. MAbs. 2017;9(1):114–26. doi: 10.1080/19420862.2016.1249079. [PubMed: 27786612]
12. Cho BC, Lee J-S, Han J-Y, Cho EK, Haura E, Lee KH, et al. 1497PJNJ-61186372 (JNJ-372), an EGFR-cMET bispecific antibody, in advanced non-small cell lung cancer (NSCLC): An update on phase I results. Annals of Oncology. 2018;29(suppl_8). doi: 10.1093/annonc/mdy292.118.
13. de Matos LL, Trufelli DC, de Matos MGL, da Silva Pinhal MA. Immunohistochemistry as an Important Tool in Biomarkers Detection and Clinical Practice. Biomark Insights. 2010;5:9–20. [PubMed: 20212918]
14. Penault-Llorca F, Viale G. Pathological and molecular diagnosis of triple-negative breast cancer: a clinical perspective. Ann Oncol. 2012;23 Suppl 6:vi19–22. doi: 10.1093/annonc/mds190. [PubMed: 23012297]
15. Pozner-Moulis S, Cregger M, Camp RL, Rimm DL. Antibody validation by quantitative analysis of protein expression using expression of Met in breast cancer as a model. Lab Invest. 2007;87(3):251–60. doi: 10.1038/labinvest.3700515. [PubMed: 17260003]
16. Knudsen BS, Zhao P, Resau J, Cottingham S, Gherardi E, Xu E, et al. A novel multipurpose monoclonal antibody for evaluating human c-Met expression in preclinical and clinical settings. Appl Immunohistochem Mol Morphol. 2009;17(1):57–67. doi: 10.1097/PAI.0b013e3181816ae2. [PubMed: 18815565]
17. McKnight BN, Viola-Villegas NT. 89Zr-ImmunoPET Companion Diagnostics and their Impact in Clinical Drug Development. J Labelled Comp Radiopharm. 2018;61(9):727–38. doi: 10.1002/jlcr.3605. [PubMed: 29341222]
18. Radiopharmaceutical Chemistry | Lewis Jason S. | Springer 2019.
19. McKnight BN, Kuda-Wedagedara ANW, Sevak KK, Abdel-Atti D, Wiesend WN, Ku A, et al. Imaging EGFR and HER3 through 89 Zr-labeled MEHD7945A (Duligotuzumab). Scientific Reports. 2018;8(1):1–13. doi: doi:10.1038/s41598-018-27454-6. [PubMed: 29311619]
20. Moek KL, Waaijer SJH, Kok IC, Suurs FV, Brouwers AH, Oordt CWM-vdHv, et al. 89Zr-labeled Bispecific T-cell Engager AMG 211 PET Shows AMG 211 Accumulation in CD3-rich Tissues and Clear, Heterogeneous Tumor Uptake. Clin Cancer Res. 2019. doi: 10.1158/1078-0432.CCR-18-2918.
21. Kim EM, Jeong MH, Kim DW, Jeong HJ, Lim ST, Sohn MH. Iodine 125-labeled mesenchymal-epithelial transition factor binding peptide-click-cRGDyk heterodimer for glioma imaging. Cancer Sci. 2011;102(8):1516–21. doi: 10.1111/j.1349-7006.2011.01983.x. [PubMed: 21575108]
22. Robinson MK, Hodge KM, Horak E, Sundberg ÅL, Russeva M, Shaller CC, et al. Targeting ErbB2 and ErbB3 with a bispecific single-chain Fv enhances targeting selectivity and induces a therapeutic effect in vitro. Br J Cancer. 2008;99(9):1415–25. doi: 10.1038/sj.bjc.6604700. [PubMed: 18841159]
23. Luo H, Hong H, Yang SP, Cai W. Design and Applications of Bispecific Heterodimers: Molecular Imaging and beyond. Mol Pharm. 2014;11(6):1750–61. doi: 10.1021/mp500115x. [PubMed: 24738564]
24. Marquez-Nostra BV, Lee S, Laforest R, Vitale L, Nie X, Hyrc K, et al. Preclinical PET imaging of glycoprotein non-metastatic melanoma B in triple negative breast cancer: feasibility of an antibody-based companion diagnostic agent. Oncotarget. 2017;8(61):104303–14. doi: 10.18632/oncotarget.22228. [PubMed: 29262642]

Author Manuscript Author Manuscript Author Manuscript Author Manuscript

25. Encarnação JC, Barta P, Fornstedt T, Andersson K. Impact of assay temperature on antibody binding characteristics in living cells: A case study. Biomed Rep. 2017;7(5):400–6. doi: 10.3892/br.2017.982. [PubMed: 29181152]

26. Abou D, Ku T, Smith-Jones P. In vivo biodistribution and accumulation of 89Zr in mice. Nucl Med Biol. 2011;38(5):675–81. doi: 10.1016/j.nucmedbio.2010.12.011. [PubMed: 21718943]

Author Manuscript Author Manuscript Author Manuscript Author Manuscript

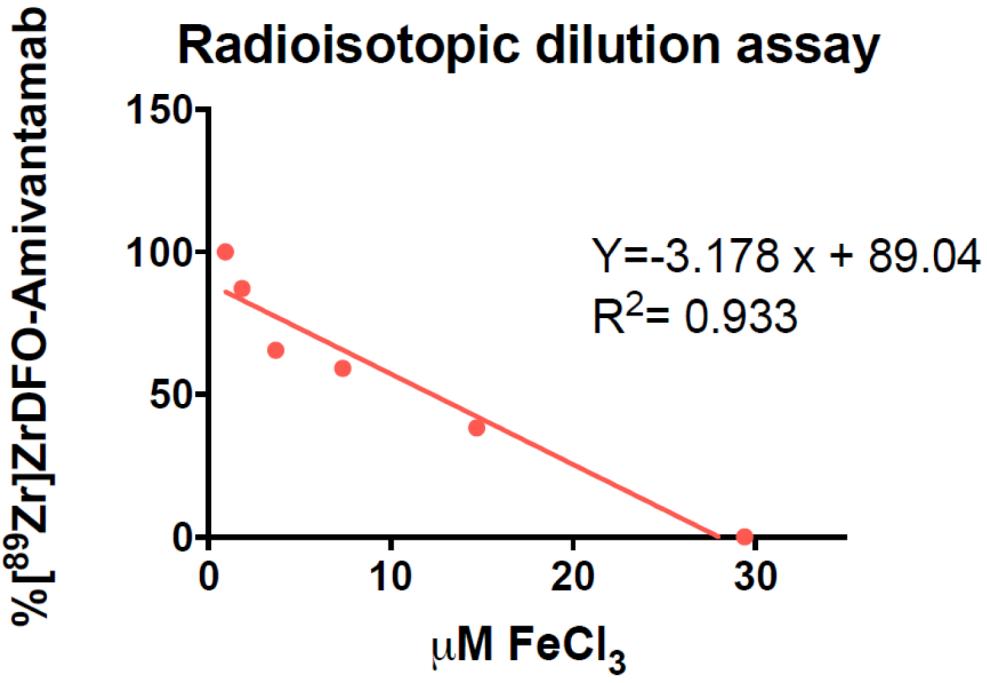

Fig. 1.

Representative graph of the radioisotopic dilution assay to determine the ratio DFO: Amivantamab. The number of the DFO per antibody was found to be 5 ± 1 (n = 3 experimental replicates)

Author Manuscript Author Manuscript Author Manuscript Author Manuscript

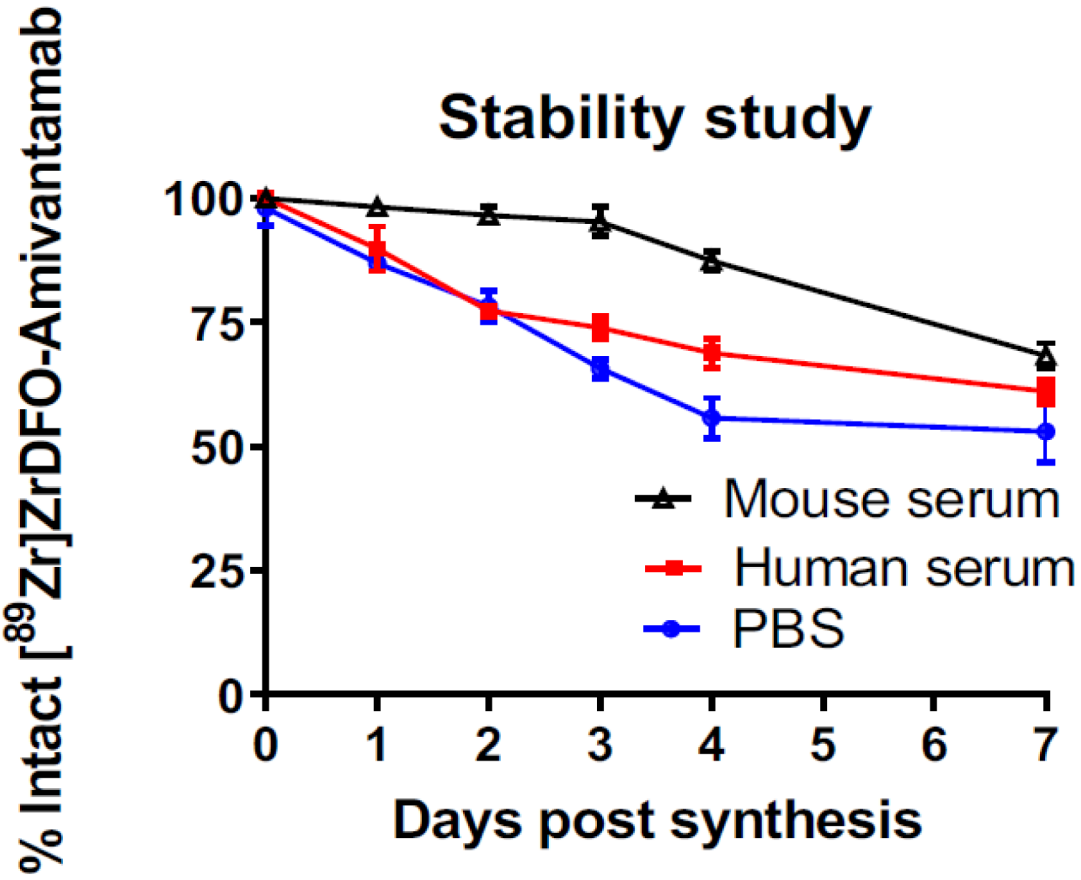

Fig. 2.

Stability of [^{89}Zr]ZrDFO-Amivantamab in PBS at ambient temperature and in mouse and human sera at 37°C (n = 3 replicates each)

Author Manuscript Author Manuscript Author Manuscript Author Manuscript

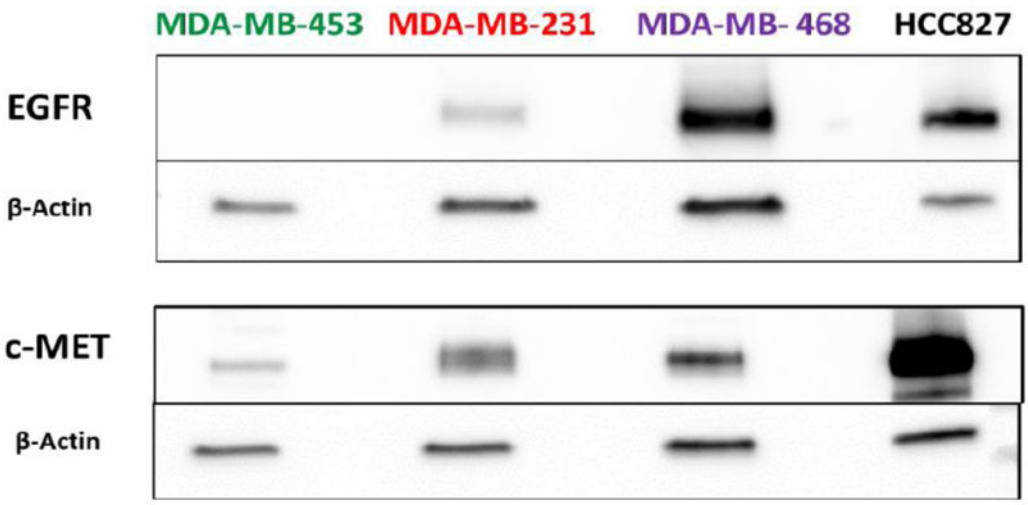

Fig. 3.

In vitro validation of EGFR and c-MET expression in TNBC cell lines via Western blot analysis

Author Manuscript
Author Manuscript
Author Manuscript
Author Manuscript

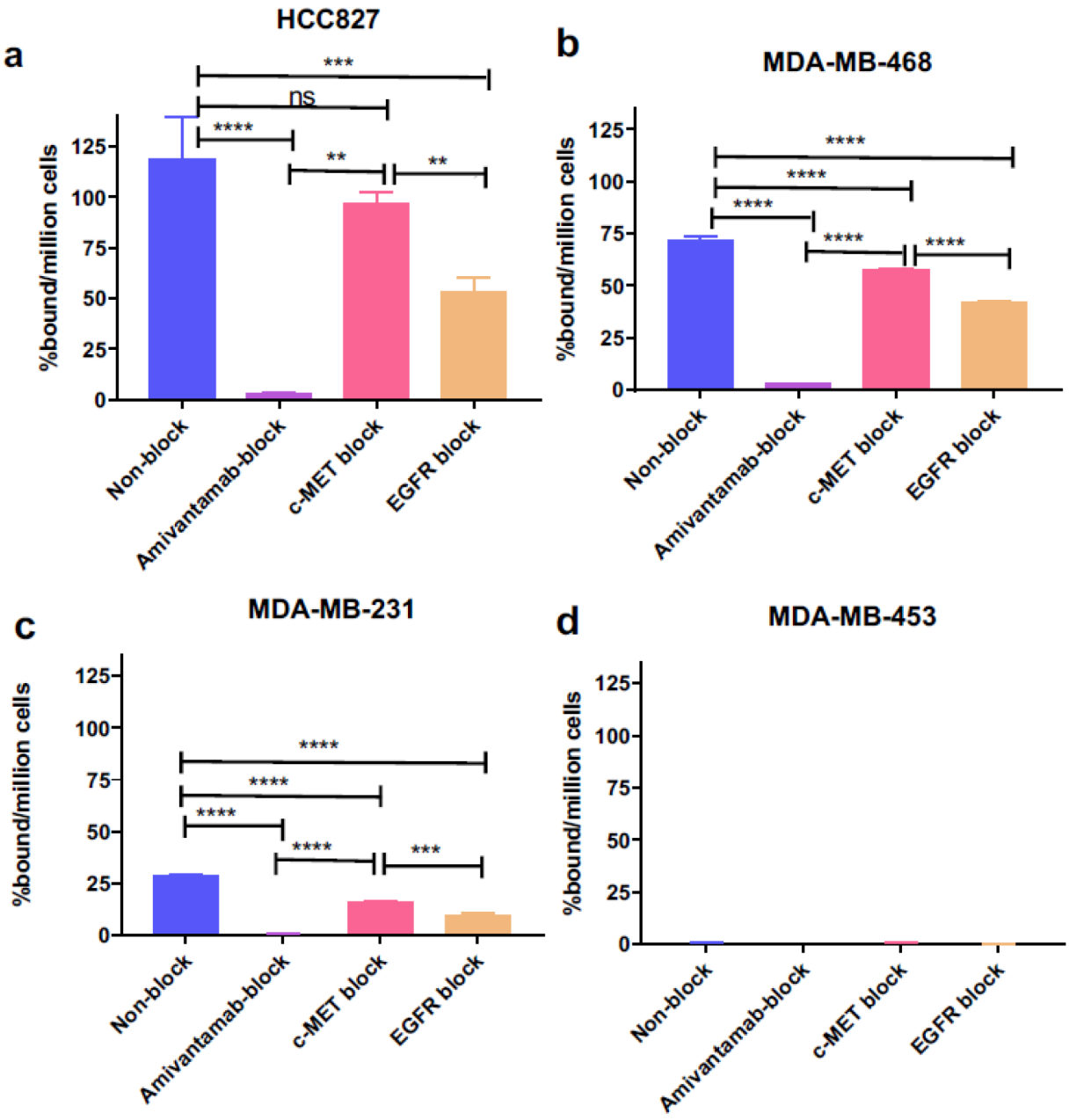

Fig. 4.

[^{89}Zr]ZrDFO-Amivantamab binding (Baseline) and blocking with 200-fold excess unlabeled Amivantamab (Amivantamab block), single arm α-EGFR (EGFR block), and single arm α-c-MET (c-MET block) in HCC827 (**a**) (n = 3 replicates each; *** $p < 0.001$, **** $p < 0.0001$)

Author Manuscript Author Manuscript Author Manuscript Author Manuscript

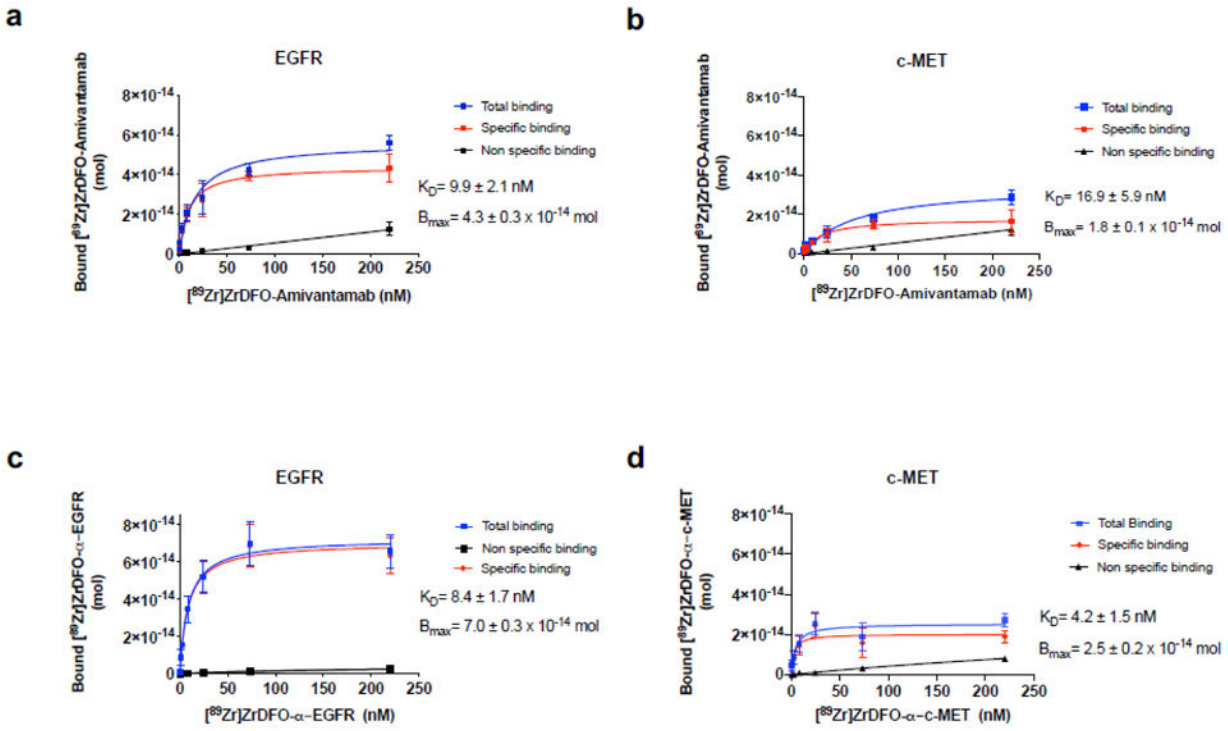

Fig. 5.

Saturation plots of ^{89}Zr-labeled antibodies to determine binding affinity (Kd). [^{89}Zr]ZrDFO-Amivantamab to EGFR (**a**) and c-MET (**b**) proteins, [^{89}Zr]ZrDFO-α-EGFR to EGFR protein (**c**) and [^{89}Zr]ZrDFO-α-c-MET to c-MET proteins (**d**) (n = 3 replicates each)

Author Manuscript Author Manuscript Author Manuscript Author Manuscript

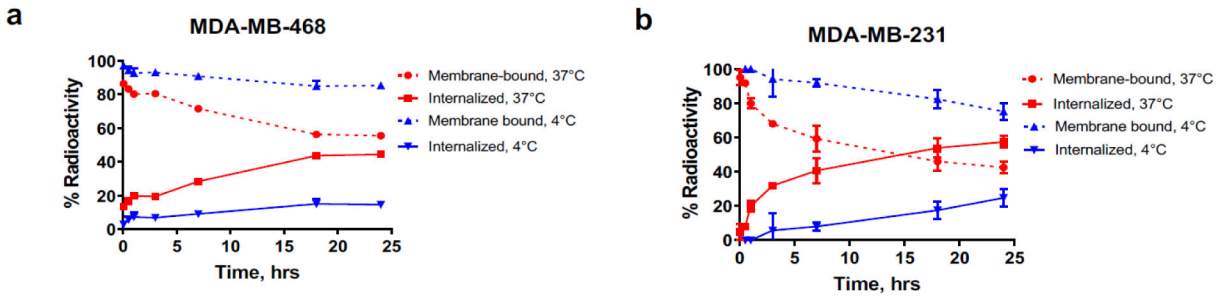

Fig. 6.

Cell internalization rate of [^{89}Zr]ZrDFO-Amivantamab in the MDA-MB-468 (**a**) and MDA-MB-231 (**b**) lines at 37°C and at 4°C (n = 3 replicates each)

Author Manuscript Author Manuscript Author Manuscript Author Manuscript

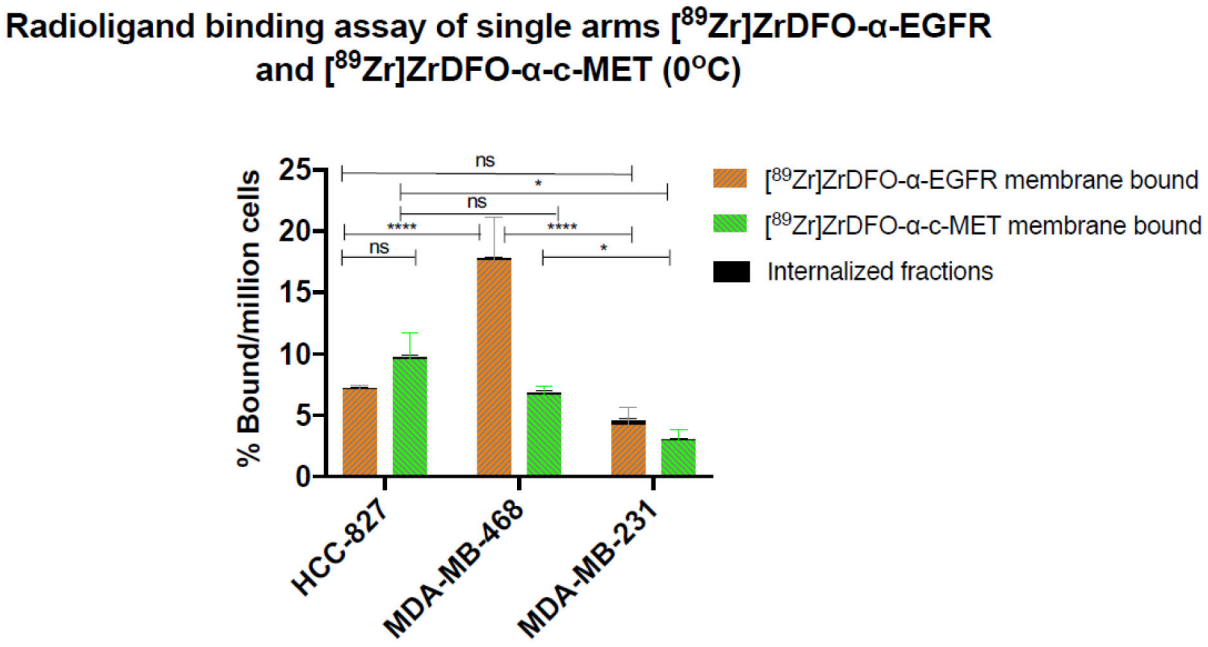

Fig. 7.

In vitro validation of EGFR and c-MET membrane expression in TNBC cell lines using [^{89}Zr]ZrDFO-α-EGFR and [^{89}Zr]ZrDFO-α-c-MET. No significant internalization of the probes (< 0.1%) is observed across the cell lines (n = 3 replicates each; * $p < 0.05$, **** $p < 0.0001$)

Author Manuscript Author Manuscript Author Manuscript Author Manuscript

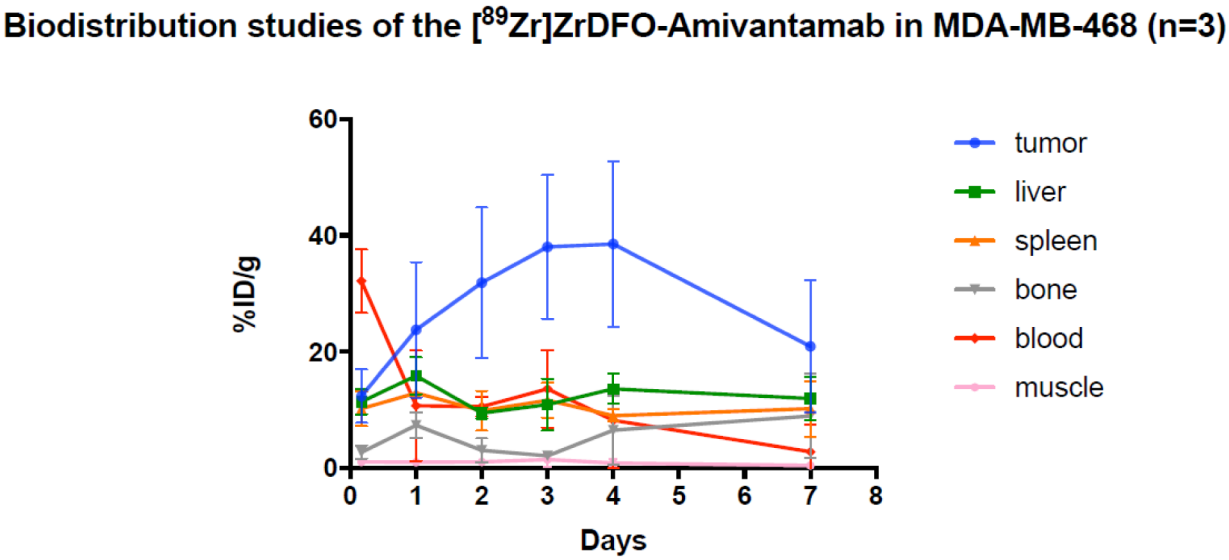

Fig. 8.

Whole-body biodistribution of [^{89}Zr]ZrDFO-Amivantamab from 6 h to 7 days p.i. (n = 3 per group)

Author Manuscript Author Manuscript Author Manuscript Author Manuscript

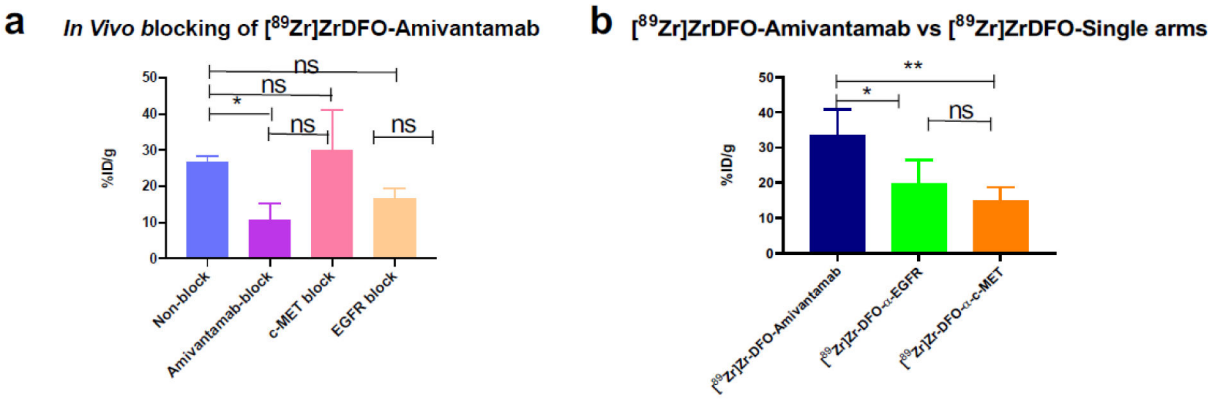

Fig. 9.

Binding specificity of [^{89}Zr]ZrDFO-Amivantamab (0.37 MBq = 2.5 μg) *in vivo* determined by biodistribution studies at 4 days p.i in the MDA-MB-468 xenograft model, was evaluated 4 days p.i. (**a**) [^{89}Zr]ZrDFO-Amivantamab uptake in the tumor under baseline and blocking conditions with 20 mg/kg of Amivantamab, α-EGFR, or α-c-MET (n = 3 per group); (**b**) Comparison of tumor uptake among [^{89}Zr]ZrDFO-Amivantamab, [^{89}Zr]ZrDFO-α-EGFR and [^{89}Zr]ZrDFO-α-c-MET (n = 4 per group; * $p < 0.05$, ** $p < 0.01$)

Author Manuscript
Author Manuscript
Author Manuscript
Author Manuscript

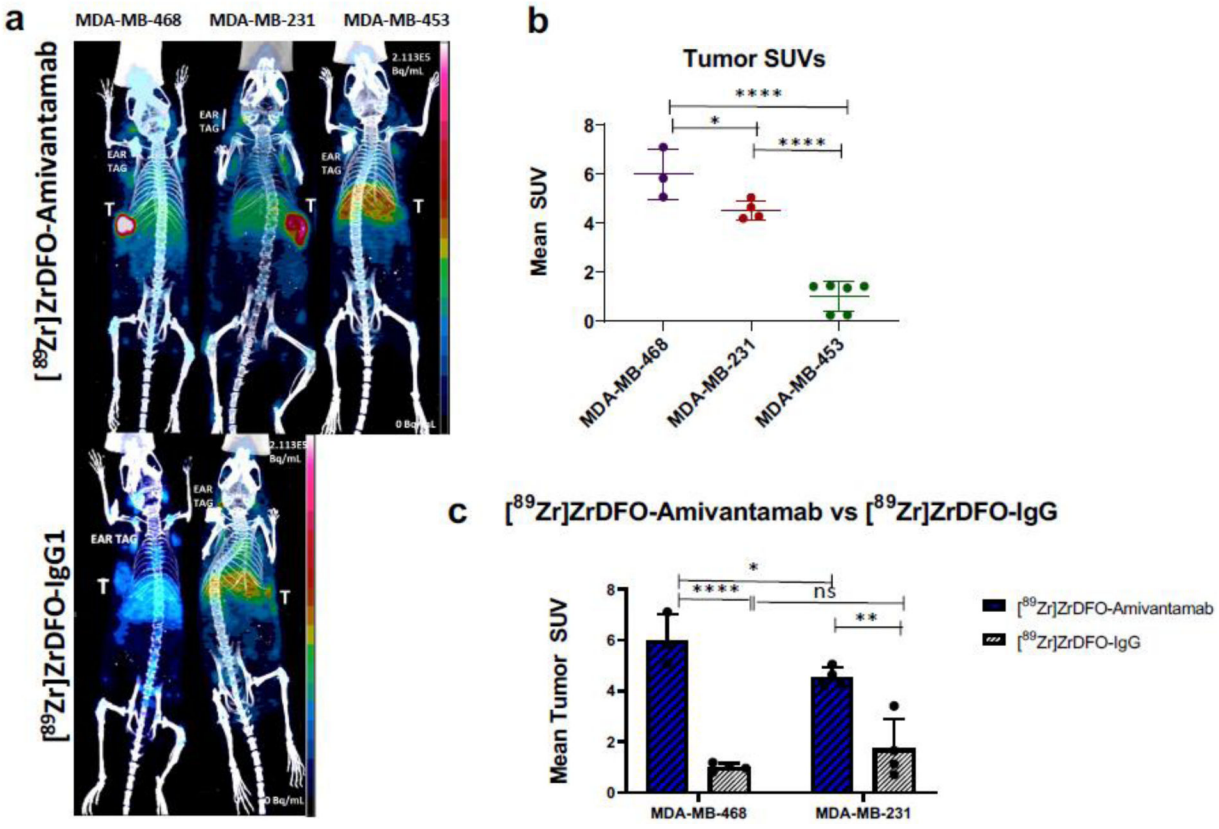

Fig. 10.

PET/CT imaging at 4 days p.i. of 1.85 MBq of either [^{89}Zr]ZrDFO-Amivantamab or [^{89}Zr]ZrDFO-IgG1 in MDA-MB-468, MDA-MB-231, and MDA-MB-453 TNBC xenografts. (**a**) Maximum Intensity Projections of representative mice (**b**) Quantification of tumor uptake of [^{89}Zr]ZrDFO-Amivantamab in MDA-MB-468 (n = 3), MDA-MB-231 (n = 4) and MDA-MB-453 (n = 6) xenografts. (**c**) Comparison of tumor uptake between [^{89}Zr]ZrDFO-Amivantamab and [^{89}Zr]ZrDFO-IgG1 in MDA-MB-468 and in MDA-MB-231 tumors (n = 3 per group; * $p < 0.05$, ** $p < 0.01$, **** $p < 0.0001$)

Author Manuscript Author Manuscript Author Manuscript Author Manuscript

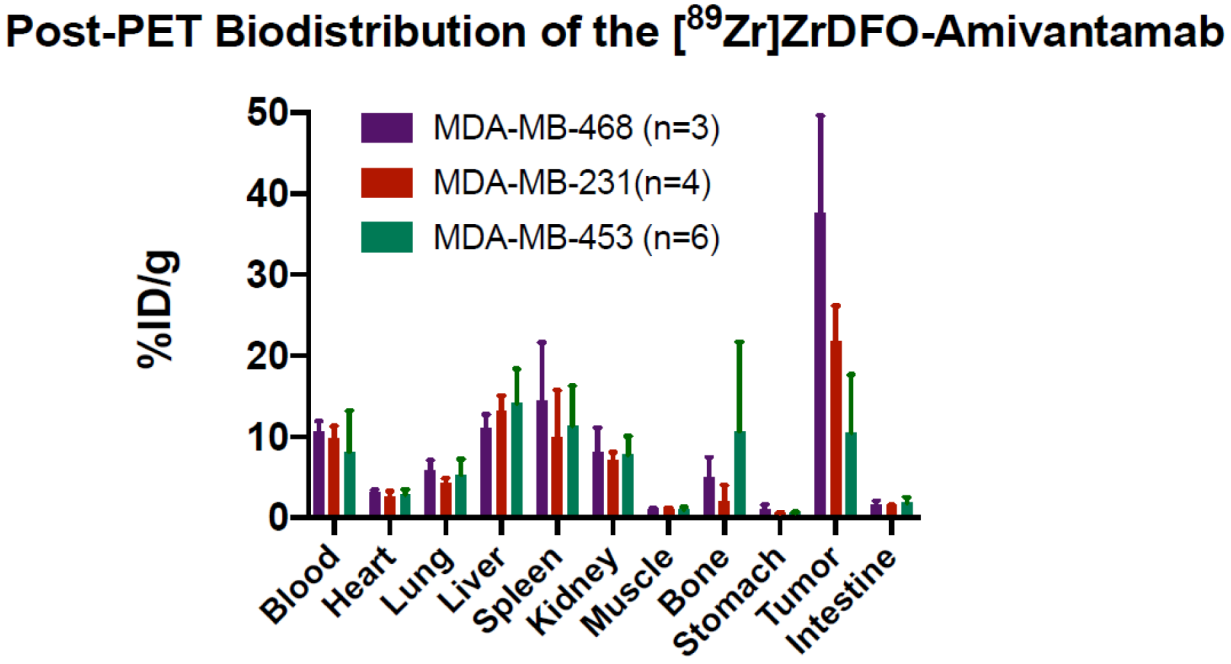

Fig. 11.

Post-PET biodistribution at 4 days p.i. of [^{89}Zr]ZrDFO-Amivantamab in mice bearing the MDA-MB-468, MDA-MB-231 and MDA-MB-453 xenografts

Author Manuscript Author Manuscript Author Manuscript Author Manuscript

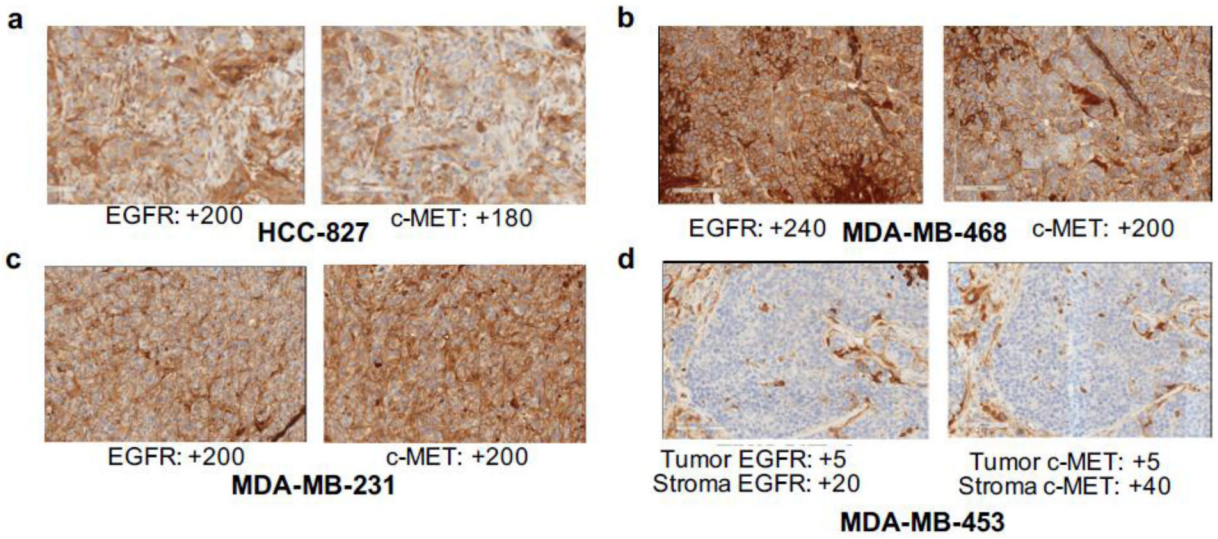

Fig. 12.

Ex vivo validation of EGFR and c-MET expression in HCC827 (**a**), MDA-MB-468 (**b**), MDA-MB-231 (**c**) and MDA-MB-453 (**d**) tumor sections via IHC. Brown stain represents receptor expression and blue counterstain represents nuclear staining (hematoxylin). Values represent H-scores, which were analyzed by board-certified pathologists